

SPINNING MOTIONS IN CORONAL CAVITIES

Y.-M. WANG AND G. STENBORG¹

Space Science Division, Naval Research Laboratory, Washington, DC 20375-5352, USA; yi.wang@nrl.navy.mil, guillermo.stenborg.ctr.ar@nrl.navy.mil
 Received 2010 June 17; accepted 2010 July 5; published 2010 August 3

ABSTRACT

In movies made from Fe XII 19.5 nm images, coronal cavities that graze or are detached from the solar limb appear as continually spinning structures, with sky-plane projected flow speeds in the range 5–10 km s^{−1}. These whirling motions often persist in the same sense for up to several days and provide strong evidence that the cavities and the immediately surrounding streamer material have the form of helical flux ropes viewed along their axes. A pronounced bias toward spin in the equatorward direction is observed during 2008. We attribute this bias to the poleward concentration of the photospheric magnetic flux near sunspot minimum, which leads to asymmetric heating along large-scale coronal loops and tends to drive a flow from higher to lower latitudes; this flow is converted into an equatorward spinning motion when the loops pinch off to form a flux rope. As sunspot activity increases and the polar fields weaken, we expect the preferred direction of the spin to reverse.

Key words: Sun: corona – Sun: coronal mass ejections (CMEs) – Sun: filaments, prominences – Sun: magnetic topology – Sun: surface magnetism – Sun: UV radiation

Online-only material: animations

1. INTRODUCTION

Coronal cavities (also known as prominence/filament cavities/channels) are tunnel-like regions of reduced electron density which enclose prominences/filaments and are aligned with polarity inversion lines (PILs) of the photospheric magnetic field. When observed at the solar limb in white light, in the coronal green and red lines, in the extreme ultraviolet (EUV), and in soft X-rays, they appear as relatively dark, semicircular or circular regions underneath coronal streamers (Waldmeier 1970; Saito & Tandberg-Hanssen 1973; Serio et al. 1978). The densities in the cavities are typically ~30% lower than that of the adjacent streamer material, with the difference decreasing with height (Fuller et al. 2008; Fuller & Gibson 2009). According to the local differential emission measure analysis of Vásquez et al. (2009), the cavities are on average somewhat hotter than the streamers and are characterized by a greater spread in temperatures.

The physical nature of prominences and their cavities is a subject of much ongoing debate (see the review of Mackay et al. 2010). While it remains unclear whether prominences have the structure of a helical flux rope or a sheared arcade that is eventually converted into a flux rope by magnetic reconnection processes, it is generally agreed that they contain a strong axial field component. Because the radial field component is weak in the vicinity of the PIL, total pressure balance with the surrounding streamer arcade (which is rooted in relatively strong field) requires that the coronal cavity also contain a significant axial field component. It is then natural to assume that a cavity with a semicircular cross section represents a sheared arcade with axis perpendicular to the sky plane, whereas a circular or oval cavity whose bottom grazes or lies above the limb has the topology of a helical flux rope.

It has long been recognized that prominences are not in static equilibrium and that material continually streams up and down their legs or “barbs” and along their spines at speeds of ~5–70 km s^{−1} (see, e.g., Zirker et al. 1998). Recently, Doppler

measurements by Schmit et al. (2009) have revealed line-of-sight velocities of 5–10 km s^{−1} in prominence cavities. In this Letter, we call attention to the spinning motions seen in projection against the sky plane in time-lapse movies of circular coronal cavities, consistent with the presence of ordered flows along helical flux ropes. We also note a statistical bias in the direction of the circulation and suggest that this bias is due to the poleward concentration of the photospheric magnetic field near sunspot minimum.

2. EUV OBSERVATIONS

The results of this study are based on an examination of coronal cavities observed during 2008, when sunspot activity was near its minimum. The cavities were identified in full-disk images recorded with the Extreme Ultraviolet Imager (EUVI) on the *STEREO A* and *B* spacecraft (Howard et al. 2008). In order to bring out faint structures above the limb, a multiscale wavelet transform was applied to clean and enhance the images (taken in the emission lines Fe IX/X 17.1 nm, Fe XII 19.5 nm, Fe XV 28.4 nm, and He II 30.4 nm), after subtracting out a stray-light dominated background. Rather than by averaging over time as in Stenborg et al. (2008), the background model was derived by recursively applying a low-pass filter to each individual image.

Throughout 2008, numerous coronal cavities of different shapes and sizes were seen along the east and west limbs, including both semicircular (flat bottomed) and circular/oval structures. Large, long-lived cavities were persistently present above latitude ~40°, on the equatorward side of the polar coronal holes; cavities at low latitudes tended to be smaller and shorter-lived. The higher-latitude structures were located above the Sun-encircling PILs/filament channels created by rotational shearing of the photospheric field; they thus remained in the line of sight for longer periods than the low-latitude cavities, which were associated with the patchwork of PILs running mainly in the north–south direction across the equator.

Most of the cavities that grazed or were completely detached from the limb showed coherent spinning motions about their centers. These motions, best observed in running-difference

¹ Also at Interferometrics, Inc., Herndon, VA 20171, USA.

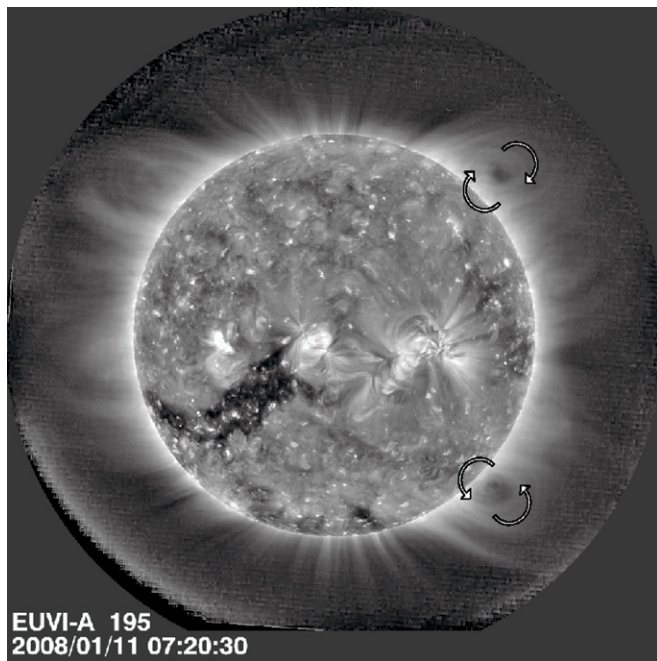


Figure 1. Wavelet-cleaned and wavelet-enhanced Fe XII 19.5 nm image recorded with EUVI A at 07:20 UT on 2008 January 11. Solar north is up and west is to the right. Dark circular cavities are clearly visible above the northwest and southwest limbs; arrows indicate the direction of the spinning motions. The continuous counterclockwise circulation of the cavity at the southwest limb during January 8–11 may be seen in the accompanying mpeg animation.

(An animation of this figure is available in the online journal.)

movies, often persist in the same sense (clockwise or counterclockwise) for several days, but sometimes reverse their direction, due either to time-dependent fluctuations in the flow or to longitudinal variations as the cavity transits the limb. The enclosed filament material tends to spin in the same sense as the cavity, but exhibits greater temporal fluctuations (especially during the eruptive process). The overlying streamer loops also show systematic flows from one footpoint to the other, in the same direction as the flows in the upper half of the cavity.

As an illustrative example, Figure 1 displays a wavelet-enhanced Fe XII 19.5 nm image taken with EUVI A on 2008 January 11. While a number of other cavities are present at both limbs, we focus on the dark circular structures that are clearly visible above the northwest limb at latitude $L \sim +45^\circ$ and above the southwest limb at $L \sim -45^\circ$. Both of these structures and the surrounding coronal material undergo continual spinning motions; the rotation is clockwise for the northern-hemisphere cavity and counterclockwise for the southern-hemisphere cavity (see the accompanying online animation). Since the “whorls” have a radius of order $0.1 R_\odot$ and complete a circuit in $\lesssim 1$ day, the corresponding flow speeds (projected onto the sky plane) are in the range $\sim 5\text{--}10 \text{ km s}^{-1}$.

From an inspection of running-difference movies made from Fe XII 19.5 nm images taken between 2008 January and December, we found a strong bias in the direction of the spinning motions: in as many as $\sim 75\%$ of the (~ 100) cavities that showed such motions, the flow was directed equatorward in the upper half of the cavity and poleward in the lower half. (We refer to this sense of rotation as being “equatorward.”) The bias was most clearly seen at higher latitudes ($|L| \gtrsim 30^\circ$).

The wavelet-enhanced 19.5 nm and 17.1 nm movies revealed many ejections that involved the cavities, the enclosed filament material, and the surrounding streamer loops. The ejections take

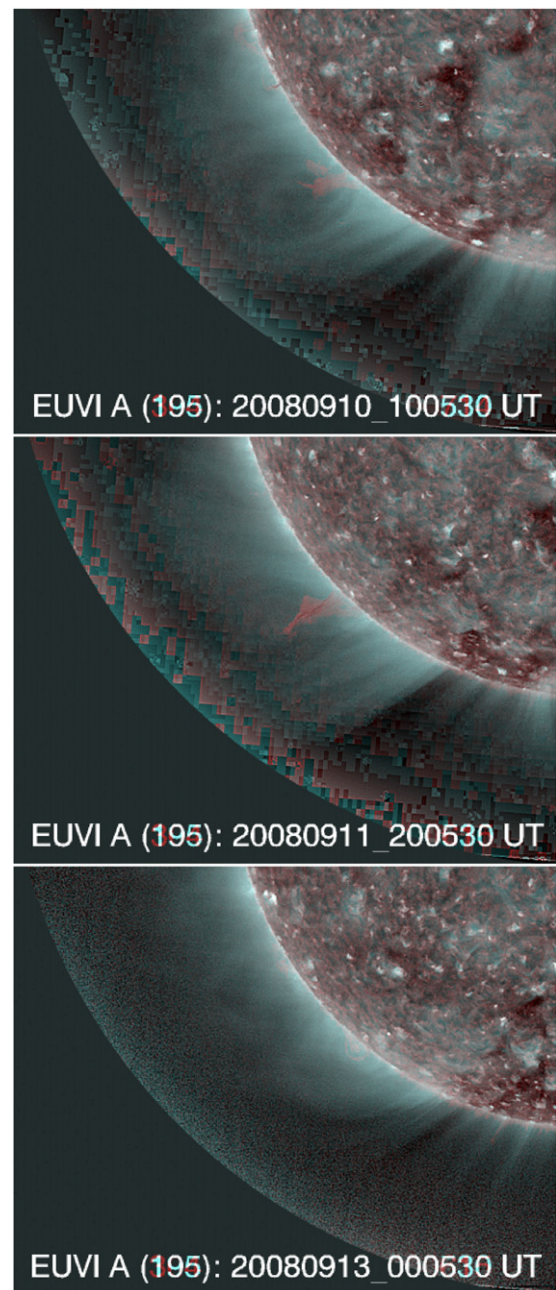


Figure 2. Composite of wavelet-enhanced Fe XII 19.5 nm (blue) and He II 30.4 nm (red) images recorded with EUVI A, showing a large circular cavity above the southeast limb at 10:05 UT on 2008 September 10 (top panel), its eruption at 20:05 UT on September 11 (middle panel), and the cavity-less post-eruption configuration at 00:05 UT on September 13 (bottom panel). As seen from the online mpeg animation constructed from 19.5 nm frames taken during September 10–11, the cavity and surrounding streamer material spin clockwise.

(An animation of this figure is available in the online journal.)

the form of elongated blobs or concave-outward flux ropes, which pinch off well above the limb and often show spinning or swirling motions (not always in the same sense as that of the pre-eruption cavity); the pinched-off material tends to be channeled equatorward by the dipole-like coronal field. In one-third to one-half of these events, slow streamer blowouts were subsequently observed by the white-light coronagraphs on *STEREO*; in the remaining cases, we found no clear evidence for associated coronal mass ejections (CMEs).

Figure 2 shows a large cavity at the southeast limb on September 10, its eruption on September 11, and the

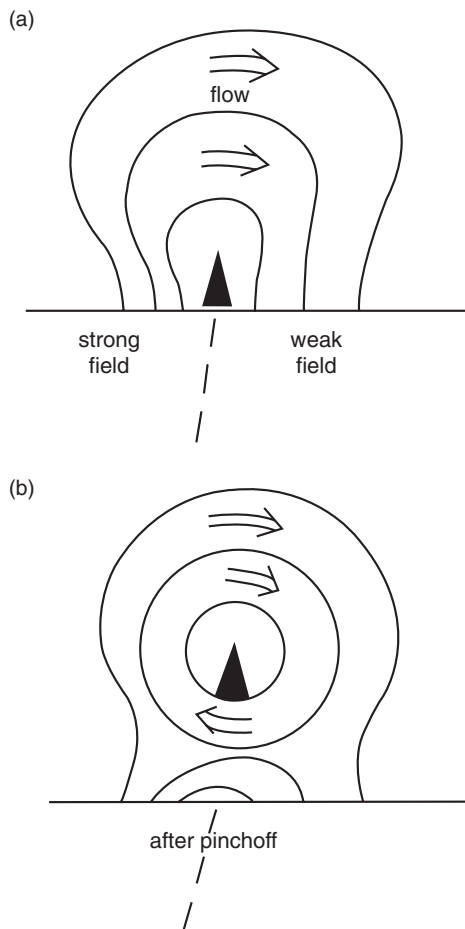


Figure 3. Mechanism for generating coherent spinning motions in coronal cavities. (a) Asymmetric heating drives a flow from the stronger- toward the weaker-field footpoints of the loop arcade overlying the filament (which itself may be a highly sheared arcade). Although not shown, a component of the magnetic field pointing perpendicular to the page is assumed to be present. (b) As the filament rises, the loops pinch off under it to form a helical flux rope, and the flow is converted into a rotary motion directed (in the upper half of the cavity) from the stronger- toward the weaker-field side of the filament channel. The flux rope remains anchored to the Sun at its far ends, located in front of and behind the plane of the page.

post-eruption streamer arcade on September 13. Here, in order to more clearly display the associated prominence, we have superposed EUVI A images taken in Fe XII 19.5 nm and He II 30.4 nm. As is evident from the accompanying online animation, the cavity and surrounding material spin clockwise (equatorward circulation). The eruption of the cavity coincides with the lifting-off of the underlying filament. A large, slow streamer blowout was observed above the east limb during September 12–13.

It should be remarked that whirling coronal cavities have long been visible in running-difference movies made from 19.5 nm images taken with the EUV Imaging Telescope (EIT) on the *Solar and Heliospheric Observatory*; to our knowledge, however, they have not previously been discussed in the literature.

3. PHYSICAL INTERPRETATION

We start from the assumption that a coronal cavity which grazes or is detached from the solar surface represents a helical flux rope viewed along its axis. The flux rope is formed as streamer loops pinch off below a slowly rising filament, which

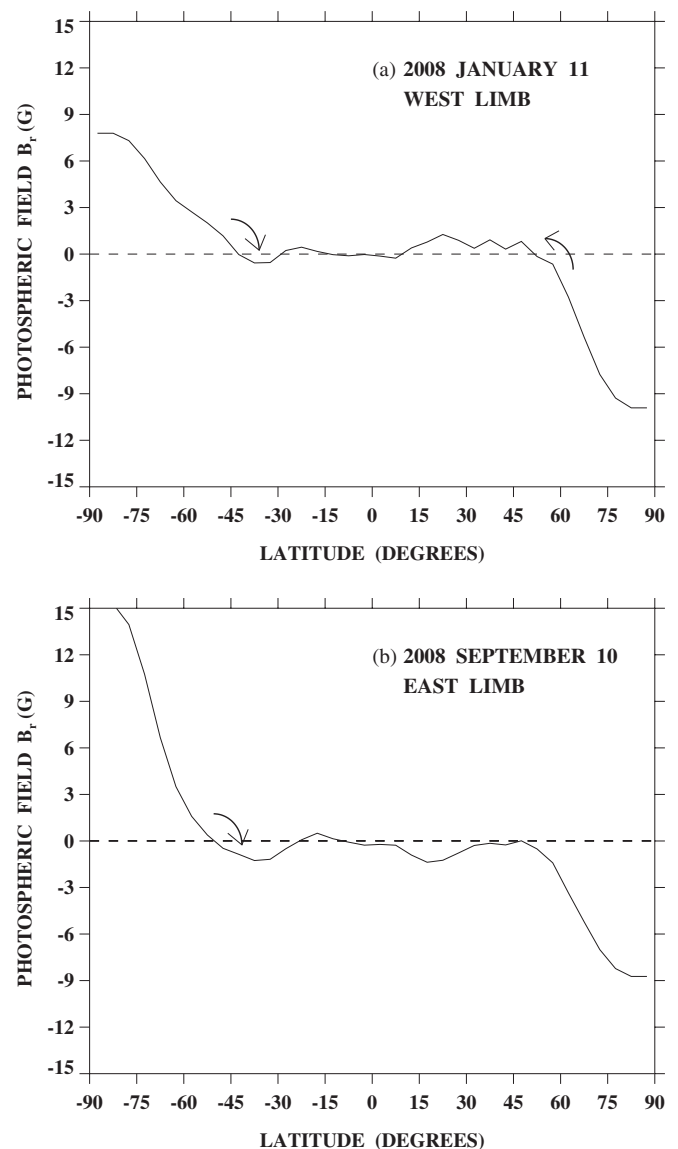


Figure 4. Poleward concentration of the photospheric magnetic flux distribution during the 2008 sunspot minimum. (a) Latitudinal variation of B_r , the radial component of the photospheric field, at the west limb on 2008 January 11. (b) Latitudinal variation of B_r at the east limb on 2008 September 10. In both cases, the field has been averaged over a 30° wide band in longitude centered on the given limb; the magnetograph measurements are from the MWO photospheric maps for CR 2065 and 2074, respectively, and have been deprojected and corrected for line profile saturation as in Wang et al. (2009). Arrows indicate the direction of flow in the (upper half of the) coronal cavities in Figures 1 and 2; the circulation in each case is directed equatorward, from the stronger- to the weaker-field side of the PIL.

originally has the form of a sheared arcade but is itself gradually converted into a twisted flux rope by reconnection processes (see, e.g., van Ballegoijen & Martens 1989).

In order to account for the observed spinning motions, let us suppose that a systematic flow from one side of the PIL to the other is present in the pre-reconnection arcade overlying the filament, as indeed suggested by our running-difference movies. Such flows might arise if the footpoint fields are stronger on one side of the PIL than the other; on the assumption that the coronal heating rate is an increasing function of the local field strength, thermal pressure gradients would then drive a siphon flow in the direction of the weaker footpoint fields (see, e.g., Winebarger et al. 2002; Sakao et al. 2007; Doschek et al. 2008). As the cavity and adjacent streamer loops pinch off to form a flux rope,

the unidirectional flow will be converted into helical motion, with the direction of circulation in the upper (lower) half of the cavity being toward the weaker (stronger) footpoint fields (see Figure 3).

This scenario suggests a simple explanation for the bias toward equatorward circulation in the cavities observed during the 2008 activity minimum. Over the course of the solar cycle, the $10\text{--}20\text{ m s}^{-1}$ surface meridional flow transports trailing-polarity flux from the active region belts to the poles, giving rise to highly concentrated polar fields near sunspot minimum; except around active regions, the longitudinally averaged photospheric field then varies with latitude roughly as $\sin^n L$, where $n \gtrsim 7$ (Svalgaard et al. 1978; Sheeley et al. 1989; Petrie & Patrikeeva 2009; Wang et al. 2009). As a consequence of this steep poleward gradient in the field strength, we would expect the heating along long coronal loops rooted in the quiet Sun to be strongest near their higher-latitude footpoints, driving an equatorward flow. In particular, the sense of circulation in large cavities containing quiescent prominences should be preferentially equatorward in the upper half of the cavity.

In Figure 4, we have plotted the latitudinal variation of the photospheric field, $B_r(L)$, at the west limb on 2008 January 11 and at the east limb on 2008 September 10. The magnetograph measurements, extracted from the Mount Wilson Observatory (MWO) synoptic maps for Carrington rotations (CRs) 2065 and 2074, have been deprojected by dividing by $\cos L$, corrected for line profile saturation, and averaged over a 30° -wide longitude band centered on the Carrington longitude of the limb. The two dark cavities above the west limb in Figure 1 are located in the vicinity of the polarity reversals at $L \sim \pm 45^\circ$ in Figure 4(a); in both hemispheres, the photospheric field strength is seen to increase more steeply on the poleward side of the PIL than on the equatorward side, consistent with the clockwise rotation of the northern-hemisphere cavity and the counterclockwise rotation of the southern-hemisphere cavity. Similarly, Figure 4(b) shows the field strength increasing more steeply on the poleward side of the PIL at $L \sim -50^\circ$, consistent with the clockwise rotation of the large cavity above the southeast limb in Figure 2.

4. CONCLUSIONS

The coherent spinning motions described here, together with the line-of-sight Doppler measurements of Schmit et al. (2009), point clearly to the presence of helical flows along circular or “detached” coronal cavities, thus supporting the assumption that these structures are helical flux ropes viewed along their axes. When observed at the limb as the Sun rotates, the whirling motions (best seen in Fe XII 19.5 nm running-difference movies) often persist in the same sense for $\sim 2\text{--}3$ days, but may also intermittently reverse their direction. The spinning structures, which include the immediately surrounding streamer material, have a characteristic radius of order $0.1 R_\odot$ and orbital period $\lesssim 1$ day, corresponding to flow speeds of $5\text{--}10\text{ km s}^{-1}$. These transverse speeds are similar to the axial (line of sight) speeds derived by Schmit et al. (2009) and are comparable to or less than the streaming velocities measured in prominences/filaments.

We have noted a remarkable bias in the direction of the spinning motions, with the flow being preferentially equatorward (in the upper half of the cavity as well as in the overlying streamer loops). We attribute this bias to the poleward concentration of the large-scale photospheric field near sunspot minimum, which causes the footpoint heating to be stronger on the poleward side of the PIL and drives a siphon flow toward the equator, which is converted into an equatorward spinning motion after the arcade loops pinch off to form a flux rope. As active regions emerge at mid-latitudes during the rising phase of cycle 24 and the polar fields are canceled by the poleward-migrating trailing-polarity flux, we might expect the preferred direction of flow to reverse, resulting in an increasing number of poleward-spinning cavities.

An obvious next step is to combine height–time measurements of sky-plane projected flows in cavities with line-of-sight Doppler observations, in order to deduce the three-dimensional structure of the flow field within the cavity flux rope. This objective should be readily achievable by performing simultaneous measurements with the Atmospheric Imaging Assembly on the recently launched *Solar Dynamics Observatory* (SDO) and with the EUV Imaging Spectrometer on *Hinode*.

This initial study raises the possibility that spinning motions identified in EUV movies may be used to unambiguously distinguish between sheared arcades, appearing as semicircular structures without spin, and helical flux ropes. Of particular interest is the question whether coronal cavities undergo a systematic evolution from the former to the latter and thence to eruption. The three viewing angles afforded by the SDO and STEREO A and B spacecraft may make it possible to track the evolution of individual cavities (or sections of filament channels) over longer periods.

This work was supported by NASA and the Office of Naval Research.

REFERENCES

- Doschek, G. A., Warren, H. P., Mariska, J. T., Muglach, K., Culhane, J. L., Hara, H., & Watanabe, T. 2008, *ApJ*, **686**, 1362
- Fuller, J., & Gibson, S. E. 2009, *ApJ*, **700**, 1205
- Fuller, J., Gibson, S. E., de Toma, G., & Fan, Y. 2008, *ApJ*, **678**, 515
- Howard, R. A., et al. 2008, *Space Sci. Rev.*, **136**, 67
- Mackay, D. H., Karpen, J. T., Ballester, J. L., Schmieder, B., & Aulanier, G. 2010, *Space Sci. Rev.*, **151**, 333
- Petrie, G. J. D., & Patrikeeva, I. 2009, *ApJ*, **699**, 871
- Saito, K., & Tandberg-Hanssen, E. 1973, *Sol. Phys.*, **31**, 105
- Sakao, T., et al. 2007, *Science*, **318**, 1585
- Schmit, D. J., Gibson, S. E., Tomczyk, S., Reeves, K. K., Sterling, A. C., Brooks, D. H., Williams, D. R., & Tripathi, D. 2009, *ApJ*, **700**, L96
- Serio, S., Vaiana, G. S., Godoli, G., Motta, S., Pirronello, V., & Zappala, R. A. 1978, *Sol. Phys.*, **59**, 65
- Sheeley, N. R., Jr., Wang, Y.-M., & Harvey, J. W. 1989, *Sol. Phys.*, **119**, 323
- Stenborg, G., Vourlidas, A., & Howard, R. A. 2008, *ApJ*, **674**, 1201
- Svalgaard, L., Duvall, T. L., Jr., & Scherrer, P. H. 1978, *Sol. Phys.*, **58**, 225
- van Ballegoijen, A. A., & Martens, P. C. H. 1989, *ApJ*, **343**, 971
- Vázquez, A. M., Frazin, R. A., & Kamalabadi, F. 2009, *Sol. Phys.*, **256**, 73
- Waldmeier, M. 1970, *Sol. Phys.*, **15**, 167
- Wang, Y.-M., Robbrecht, E., & Sheeley, N. R., Jr. 2009, *ApJ*, **707**, 1372
- Winebarger, A. R., Warren, H., van Ballegoijen, A., DeLuca, E. E., & Golub, L. 2002, *ApJ*, **567**, L89
- Zirker, J. B., Engvold, O., & Martin, S. F. 1998, *Nature*, **396**, 440